Characterization of copper-containing catalysts by $^{63/65}$Cu solid-state NMR

Spectroscopic background: ^{63}Cu and ^{65}Cu nuclei with a spin of I = 3/2, natural abundances of 69.15 % and 30.85 %, resonance frequencies of ν_0 = 132.61 and 142.96 MHz at B_0 = 11.75 T, and sensitivities of 6.5 x 10^{-2} and 3.5 x 10^{-2} in comparison with ^{1}H nuclei (1.0), respectively. These properties make the ^{63}Cu and ^{65}Cu isotopes suitable candidates for solid-state NMR spectroscopy. Due to the quadrupole moments of Q = -22.0 x 10^{-30} m^2 for ^{63}Cu and Q = -20.4 x 10^{-30} m^2 for ^{65}Cu nuclei, their quadrupole coupling constants C_Q are large and similar at analogous structural sites. In the case of ^{63}Cu solid-state NMR studies, the very similar resonance frequency of ^{23}Na nuclei (ν_0 = 132.29 MHz at B_0 = 11.75 T) may lead to an overlap of the spectral ranges of these two nuclei. For basic principles of solid-state NMR, see lectures “Solid-State NMR Spectroscopy” for Bachelor students or PhD seminars, accessible via the link “Lectures for Students”.

While **Cu^{1+} species (Cu(I)) with 3*d* ^{10} configuration are diamagnetic** and accessible for $^{63/\&5}$Cu solid-state NMR, **Cu^{2+} species (Cu(II) are paramagnetic** and accessible for ESR spectroscopy. **Cu^0 species in metallic copper nanoparticles** give $^{63/\&5}$Cu solid-state NMR signals, which show a large **Knight shift ($\Delta\delta_{63/65Cu}$ ≅ 2,000 ppm)**. Copper nanoparticles as well as Cu(I) and Cu(II) species have attracted significant attention in heterogeneous catalysis due to their high activity and selectivity, e.g. in the oxidative steam reforming of methanol, alcoholysis of cyclohexene oxide with methanol, the selective catalytic reduction (SCR) of harmful nitrogen oxides, and CO coupling reactions [1-6].

Solid-state NMR studies of **metallic Cu^0 on support materials**, such as Cu/silica [7], Cu/ZnO [8, 9], Cu/LTL [10], and Cu/TiO_2 [6], were performed via static single pulse [7] and spin echo NMR experiments [8, 9] or via single pulse MAS NMR [6, 10] spectroscopy. In the case of Cu/ZnO catalysts, utilized for the steam reforming of methanol, the influence of the **aging time of the precursor** on the state of metallic copper on the ZnO support material (**Fig. 1, left**) was investigated by static ^{63}Cu spin echo NMR [9]. The corresponding precursor consisted of copper zinc hydroxycarbonates obtained from copper and zinc nitrate solutions with sodium carbonate. The Cu/ZnO catalysts obtained by precursors aged for more than 30 min showed a significant increase in the activity compared to the catalyst obtained by the

non-aged precursor. **Fig. 1, right**, shows static ^{63}Cu spin echo NMR spectra of Cu/ZnO catalysts prepared upon a precursor aging of 0 to 120 minutes from top to bottom [9]. The spectra of the catalysts obtained from precursors aged for 0 and 15 minutes have a symmetric and narrow line profile indicating large and well-ordered copper particles at $\delta_{63Cu} \cong$ 2,000 ppm. In Ref. [10], a **downfield ^{63}Cu MAS NMR signal at δ_{63Cu} = 2,340 ppm** was assigned to **metallic copper in nanoparticles, involved in Knight shift interactions**. Sometimes, this signal overlaps with that of copper contents of the NMR probe (δ_{63Cu} = 2,330 ppm [10]), e.g., if the coil is not made by pure silver.

The spectra of the Cu/ZnO catalysts obtained from precursors aged for 30 and 120 minutes show broad signals with a line profile corresponding to small and strained copper nanoparticles. Comparison with the above-mentioned catalytic results of the steam reforming of methanol indicates that highly active Cu/ZnO catalysts contain small and strained copper nanoparticles [9].

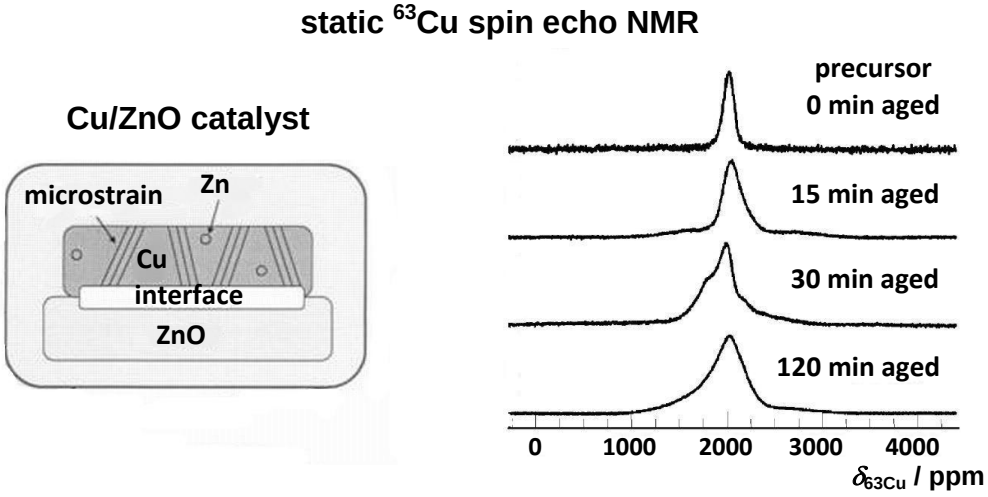

Fig. 1

Cu(I) atoms in inorganic complexes and solid catalysts were studied by solid-state NMR via different indirect and direct methods. An example for the application of an **indirect method** is the **^{13}C{^{65}Cu} transfer of population in double resonance (TRAPDOR) MAS NMR** of $CuAlCl_4$ material, modified with ethylene adducts by adsorption of ^{13}C-enriched C_2H_4 [11]. $CuAlCl_4$ containing Cu(I) atoms is utilized, e.g. supported on polymers, for the separation of olefins and CO from various feed streams [12]. The TRAPDOR pulse sequence used in Ref. [11] is shown in **Fig. 2,**

left (see also Fig. 1 in Ref. [13]). The pulse sequence in the channel of the I spins (^{13}C in the present example) consists of a spin echo experiment. If a long π pulse is additionally irradiated in the channel of the S spins (^{65}Cu in the present case) during one of the two pulse delays τ, a decrease of the echo amplitude occurs for those I spins, which interact with S spins. The difference of the echo spectra recorded with and without irradiation of the above-mentioned long π pulse gives the spectrum of I spins, which have S spins in their vicinity. The sometimes additionally applied ^{1}H decoupling improves the resolution of the echo spectrum. The values of N_{rot} correspond to the numbers of magic angle spinning periods.

Fig. 2, right, shows ^{13}C{^{65}Cu} TRAPDOR MAS NMR spectra of ethylene adducts at $CuAlCl_4$ [11]. The evaluation of the difference spectrum (**Fig. 2, right, bottom**) yielded a TRAPDOR fraction of ca. 20% for the ^{13}C MAS NMR signal of ^{13}C-enriched ethylene carbon atoms at δ_{13C} = 109 ppm. This TRAPDOR fraction hints at a strong ^{13}C-^{65}Cu dipolar coupling and ethylene-copper binding for a corresponding content of ^{13}C atoms in ethylene adducts [11].

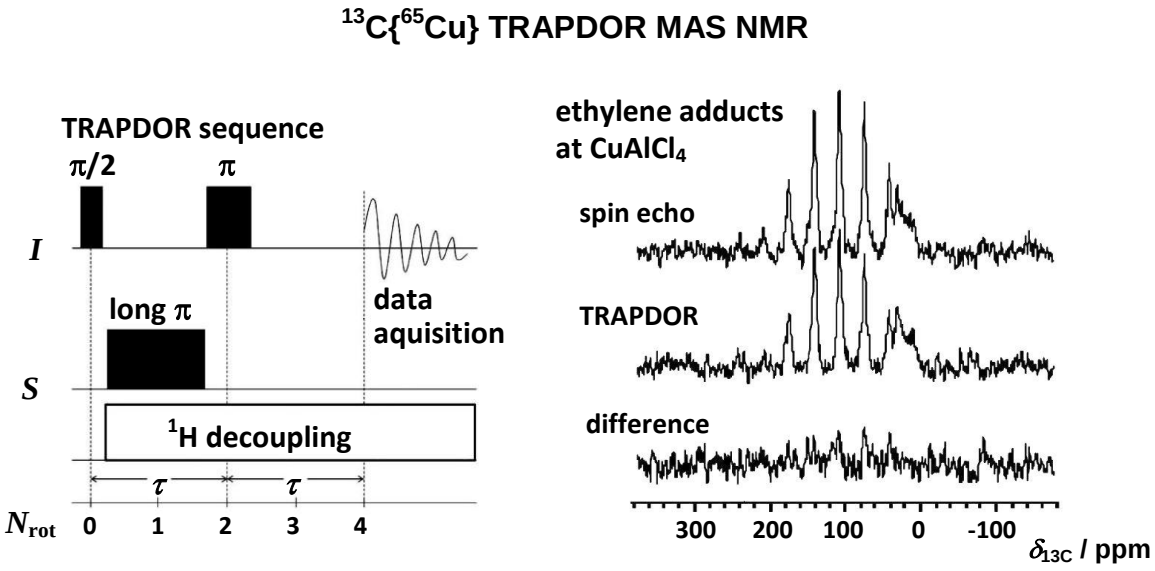

Fig. 2

Another pulse sequence, which is very similar to that in **Fig. 2, left**, is the **spin-echo double-resonance (SEDOR)** experiment. In the SEDOR sequence, the long π pulse in the channel of the S spins is replaced by a short π pulse. This π pulse is irradiated at the time t_1 after the start of the first τ window [14]. In Ref. [14], the I spins are **directly observed ^{65}Cu nuclei** and the S spins are ^{27}Al nuclei of Cu-exchanged

ZSM-5 catalysts, i.e. a **MFI-type zeolite with Cu(I) cations** (Cu^+). Two constant values of τ (200 and 350 µs) were used in the ^{65}Cu channel, while the timing t_1 of the single π pulse in the ^{27}Al channel was varied. Via **Eq. (1)** [14]:

$$(S_{\text{echo}} - S(t_1))/S_{\text{echo}} = 1 - {}^1/_2\int_0^{\pi} \cos[\omega_D 2t_1] \sin\theta \, d\theta \qquad (1)$$

the SEDOR fraction is calculated, where S_{echo} and $S(t_1)$ are the echo intensities without and with π pulse irradiation in the ^{27}Al channel, respectively. The parameter ω_D corresponds to the dipolar coupling constant D [14]:

$$D = \gamma_I \gamma_S \hbar / 2\pi r^3 \qquad (2)$$

with the gyromagnetic ratios γ_I and γ_S of the I and S spins, respectively, while Θ is the angle between the internuclear vector and the z-direction of magnetic B_0 field. Analytical solutions and algorithms for assessing the ^{65}Cu-^{27}Al distance r are described in Ref. [15]. By utilizing the SEDOR technique, in combination with **Eqs. (1) and (2)**, an **internuclear distance between the ^{65}Cu and ^{27}Al atoms** in Cu-exchanged ZSM-5 zeolite of ***r* = (0.23 ± 0.02) nm** was determined [14].

An interesting experimental tool is the temperature-dependent resonance shift of the **directly observed ^{63}Cu solid-state NMR signals of Cu(I) salts**. For Cu(I) bromide (Cu(I)Br) and Cu(I) iodide (Cu(I)I), temperature controlled solid-state phase transitions and linear chemical shift effects were observed by ^{63}Cu **variable-temperature MAS NMR (VT MAS NMR)** [16]. Upon heating of **Cu(I)Br**, a transition

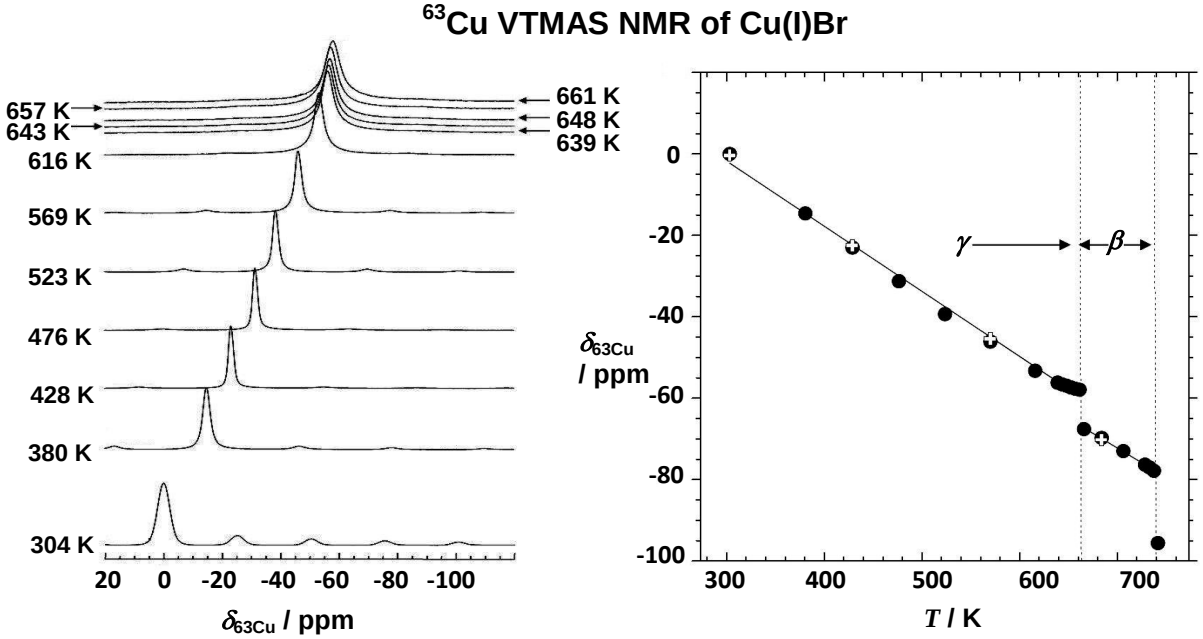

Fig. 3

from the low-temperature γ- to the high-temperature β-phase occurs at T = 661 K. In the temperature range of T = 304 to 661 K (see **Fig. 3**), typical for the γ-phase of Cu(I)Br, the following **linear relationship between the temperature T (in K) and the ^{63}Cu resonance shift $\Delta\delta_{63Cu}$** (in ppm) was found [16]:

$$\Delta\delta_{63Cu} = 64.24 - 0.16 \cdot T \qquad (3)$$

The shift values in **Eq. (3)** were determined relative to the chemical shift of Cu(I)Br at room temperature (δ_{63Cu} = 0 ppm). Similar relationships were observed for the β-phase of Cu(I)Br as well as for the γ-, β-, and α-phases of Cu(I)I [16]. These relationships are useful for the temperature calibration of NMR probes, i.e., the above-mentioned Cu(I) salts can be utilized as **NMR thermometers**, such as for *in situ* solid-state NMR studies of heterogeneously catalysed reactions at elevated temperatures.

Organometallic Cu(I) complexes, e.g. CuI(bpy)], [Cu_2I_2(bpy)], [Cu_4I_4(DABCO)$_2$] etc., are important components of crystalline metal-organic frameworks (MOFs) [17, 18]. Experimental methods for **direct $^{63/65}$Cu solid-state NMR studies** of the nature and local structure of copper atoms in these complexes [19-21] and in MOFs [17, 18] base on static solid echo [17, 18] as well as static WURST-QCPMG and QCPMG pulse sequences (see Fig. 2 of "method 17") [19-21]. As an example, **Fig. 4** shows the static ^{65}Cu QCPMG (**bottom**) and static ^{65}Cu WURST-QCPMG NMR spectra (**middle**) of pure [$(PPh_3)_2$Cu(I)O_2CPh] complexes (Fig. 3b of Ref. [20]).

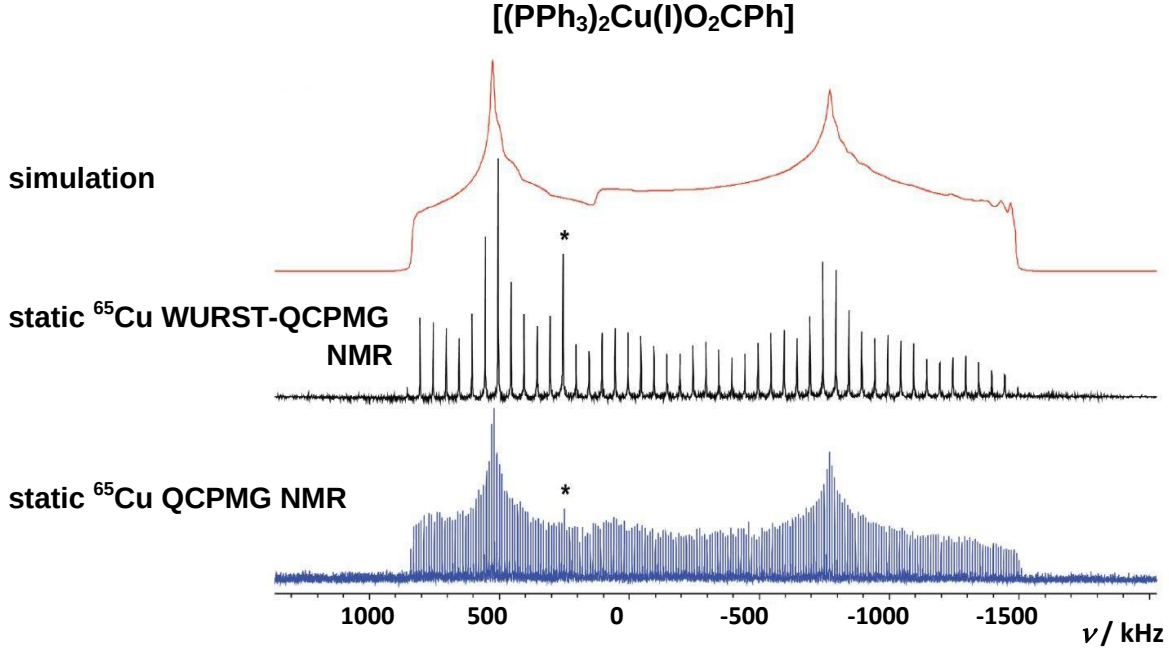

Fig. 4

Independent on the utilized pulse sequence, very similar envelops of the spikelet amplitudes are visible in **Fig. 4, middle and bottom**. These shapes of the envelops are mainly described by the quadrupolar interactions of the ^{65}Cu nuclei (spin I = 3/2) with their environment (see page 7 of the lecture “Solid-State NMR Spectroscopy” for Bachelor students, accessible via the link “Lectures for Students”). The simulation of these envelops (**Fig. 4, top**) yielded a quadrupole coupling constant of C_Q = -40.3 MHz and an asymmetry parameter of η_Q = 0.29 [20]. A survey on the experimental and calculated (Gaussian 03) parameters of the electric field gradient tensors and resulting NMR parameters of various organometallic Cu(I) complexes is given in Table 3 of Ref. [20].

Cu(I) ions exhibit a rich coordination chemistry in [Cu]MOFs and can exist in two-, three-, and four-coordinate environments, which give rise to many structural motifs and potential applications. One of these materials is the MOF SLUG-22, which local structure is illustrated in **Fig. 5** (Fig. 7a of Ref. [17]).

local structure of the metal-organic framework SLUG-22

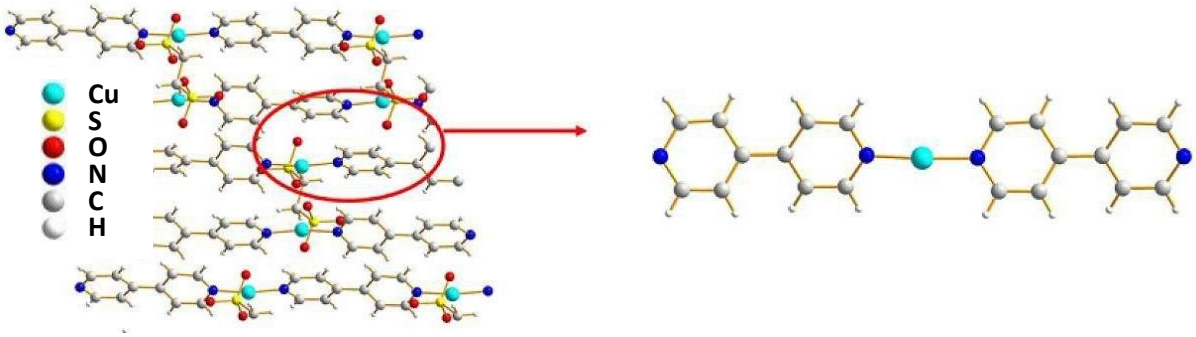

Fig. 5

The MOF SLUG-22 is composed of Cu(I)$_2$(4,4’-bpy)$_2$ units (**Fig. 5, left**), where the two-coordinate Cu(I) center is connected to two nitrogen atoms from separate 4,4’-bpy linkers in a distorted N–Cu(I)–N linear geometry, with a long-range structure consisting of one-dimensional chains of infinite length (**Fig. 5, right**). Utilizing a high magnetic field of B_0 = 21.1 T, the static ^{63}Cu and ^{65}Cu solid echo NMR spectra shown in **Fig. 6** were recorded (Figs. 7c und 7b of Ref. [17]). These spectra are extremely broad, owing to the low local symmetry of the linear two-coordinated environment at the Cu(I) atom and a correspondingly large quadrupole coupling constant C_Q. The asterisks (*) denote the signal of metallic copper (Cu^0) and the black circles (●) mark

the signal from the NMR probe background. Simulation of the envelop required the consideration of chemical shift anisotropy (CSA), but yielded only a single Cu(I) site with $C_Q(^{65}Cu)$ = 63.0 MHz and η_Q = 0.34 [17].

metal-organic framework SLUG-22

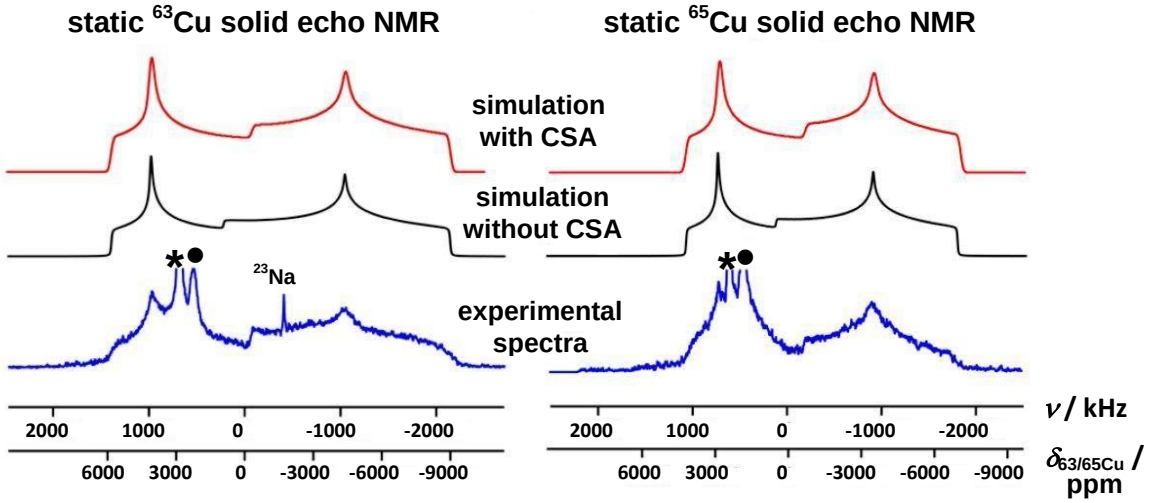

Fig. 6

Systematic studies indicated that the quadrupolar coupling constants depend on the coordination number of Cu(I) atoms [17]. A summary of the $C_Q(^{65}Cu)$ values of Cu(I)

$C_Q(^{65}Cu)$ values of Cu(I) in metal-organic coordination compounds

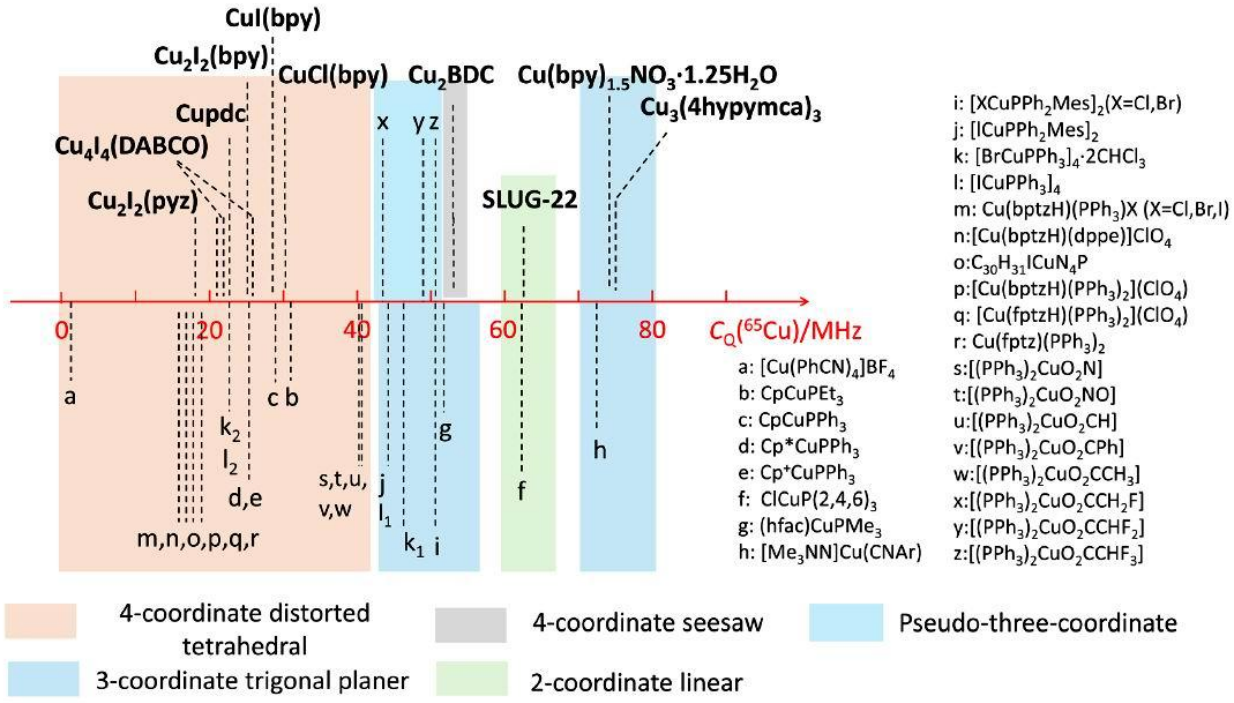

Fig. 7

atoms in [Cu]MOF and relevant metal-organic coordination compounds is illustrated in **Fig. 7** (Fig. 10 of Ref. [17]). Detailed NMR parameters are given in Table 1 of Ref. [17]. The C_Q(^{65}Cu) values of four-coordinated tetrahedral Cu(I) atoms are generally smaller than 40 MHz. The C_Q(^{65}Cu) values of three-coordinated Cu(I) atoms range from 40 MHz to 80 MHz. Four-coordinated Cu(I) atoms in a pseudo-three coordinated environment is correlated to C_Q(^{65}Cu) values between 40 and 50 MHz, which lies just between the bulk of four- and three-coordinate copper environments. A specific case is the two-coordinated Cu(I) atom in a linear environment, such as the Cu(I) atom in the MOF SLUG-22 with a C_Q(^{65}Cu) value of 63 MHz.

In the characteristic ranges of quadrupole coupling constants in **Fig. 7**, also the C_Q(^{65}Cu) values of -17.2 to -23.7 MHz for four-coordinated Cu(I) complexes, which are functionalized 3-(2′-pyridyl)-1,2,4-triazole and phosphine ligands, fit very well [24]. The above-mentioned complexes have shown potential in the preparation of photoluminescent devices [24].

Sample preparation:

The Cu/ZnO catalysts utilized for the studies shown in **Fig. 1** were measured as obtained after final calcination at T = 663 K [9] The $CuAlCl_4$ sample used for the spectra in **Fig. 2** was prepared by adsorption of double ^{13}C-labeled ethylene gas, purchased from Cambridge Isotopes, on the dried material [11]. For the VT MAS NMR studies in **Fig. 3**, commercial CuBr salt (98 %), purchased from Alfa Aesar, was used [16]. The [Cu]MOFs and metal-organic coordination compounds for the solid-state NMR studies, illustrated in **Figs. 4, 6, and 7**, were utilized as obtained after their synthesis and subsequent drying [17, 20].

$^{63/65}$Cu solid-state NMR studies:

The ^{63}Cu solid-state NMR spectra in **Fig. 1** were measured with a Bruker MSL300 spectrometer at ν_0 = 79.618 MHz (B_0 = 7.0 T) and T = 4.2 K in an Oxford cryostat. Spin echo experiments ($\pi/2$-τ_1-π) were performed with a $\pi/2$ pulse of 5.5 ms, a recycling delay of 2 s and a τ value of 25 µs. In Ref. [9], the ^{63}Cu solid-state NMR spectra are calibrated against solid CuBr at δ_{63Cu} = -381 ppm. A second reference was solid CuCl at δ_{63Cu} = -319 ppm [22].

The ^{13}C{^{65}Cu} TRAPDOR MAS NMR studies of ethylene adducts at $CuAlCl_4$ in **Fig. 2** were performed with a double-tuned Chemagnetics 5 mm probe in a CMX-360

spectrometer at resonance frequencies of ν_0 = 102.1 MHz and ν_0 = 90.5 MHz for ^{65}Cu and ^{13}C nuclei, respectively [11]. A TRAPDOR pulse sequence with ^{13}C{^{1}H} cross polarization via radio frequency fields matched at 40 kHz, a contact time of 0.5 ms, a pulse delay of 2 s, and a spinning speed of ν_{rot} = 3.0 kHz were used. The ^{13}C{^{65}Cu} TRAPDOR MAS spectra were recorded at T = 193 K [11].

The ^{63}Cu variable-temperature MAS NMR studies of Cu(I)Br in **Fig. 3** were carried out on a Varian B_0 = 14.1T spectrometer with a high-temperature MAS probe (Doty Scientific, Inc., Columbia, SC) at spinning rates of ν_{rot} = 4 kHz at room temperature and of ν_{rot} = 5 kHz at T > 373 K [16]. The spectra were collected at ν_0 = 158.94 MHz with a recycle delay of 0.5 s and a pulse length of 0.8 µs. The room temperature chemical shift of CuBr was δ_{63Cu} = -58 ppm [16].

The static ^{65}Cu QCPMG and WURST-QCPMG NMR spectra in **Fig. 4** were collected on a Varian Infinity Plus NMR spectrometer with an Oxford 9.4 T wide-bore magnet with a ^{65}Cu resonance frequency of ν_0 = 113.49 [20]. The static ultra-wideline QCPMG experiments were performed with central-transition selective $\pi/2$ pulse widths that ranged from 1.1 to 2.8 µs, optimized recycle delays from 0.15 to 0.30 s, and spectral widths of 1,000 kHz. Individual subspectra were collected by stepping the transmitter frequency across the full breadth of the powder pattern with increments between 75 and 125 kHz [20]. The WURST-QCPMG NMR experiments were performed using 50 µs WURST-80 pulses. Further details are described in Table 1 of Ref. [23].

The static ^{63}Cu solid echo NMR spectra in **Fig. 6** were obtained in a magnetic field of B_0 = 21.1 T and by recording variable-offset cumulative spectra (VOCS). The $\pi/2$ pulse width was 1 µs and a recycle delay of 0.2 s and a step size of 300 kHz were used (see Table S3 in Supporting Information of Ref. [17]).

References:

[1] K.A. Lomachenko, E. Borfecchia, C. Negri, G. Berlier, C. Lamberti, P. Beato, Hanne Falsig, S. Bordiga, *The Cu-CHA deNO$_x$ catalyst in action: Temperature-dependent NH$_3$-assisted selective catalytic reduction monitored by operando XAS and XES*, J. Am. Chem. Soc. 138 (2016) 12025-12028, DOI: 10.1021/jacs.6b06809.

[2] D.K. Pappas, K. Kvande, M. Kalyva, M. Dyballa, K.A. Lomachenko, B. Arstad, E. Borfecchia, S. Bordiga, U. Olsbye, P. Beato, S. Svelle, *Influence of Cu-speciation in mordenite on direct methane to methanol conversion: Multi-*

technique characterization and comparison with NH_3 selective catalytic reduction of NO_x, Catal. Today 369 (2021) 105-111, DOI: 10.1016/j.cattod.2020.06.050.

[3] K. Kvande, D.K. Pappas, M. Dyballa, C. Buono, M. Signorile, E. Borfecchia, K.A. Lomachenko, B. Arstad, S. Bordiga, G. Berlier, U. Olsbye, P. Beato, S. Svelle, *Comparing the nature of active sites in Cu-loaded SAPO-34 and SSZ-13 for the direct conversion of methane to methanol*, Catalysts 10 (2020) 191, DOI: 10.3390/catal10020191.

[4] J.B. Wang, C.-H. Li, T.-J. Huang, *Study of partial oxidative steam reforming of methanol over Cu–ZnO/samaria-doped ceria catalyst*, Catal. Lett. 103 (2005) 239-247, DOI: 10.1007/s10562-005-7160-8.

[5] Y. Jiang, J. Huang, M. Hunger, M. Maciejewski, A. Baiker, *Comparative studies on the catalytic activity and structure of Cu-MOF and its precursor for alcoholysis of cyclohexene oxide*, Catal. Sci. Technol. 5 (2015) 897-902, DOI: 10.1039/C4CY00916A.

[6] F. Benaskar, V. Engels, E.V. Rebrov, N.G. Patil, J. Meuldijk, P.C. Thuene, P.C.M.M. Magusin, B. Mezari, V. Hessel, L.A. Hulshof, E.J.M. Hensen, A.E. H. Wheatley, J.C. Schouten, *New Cu-based catalysts supported on TiO_2 films for Ullmann SNAr-type CO coupling reactions*, Chem. Eur. J. 18 (2012) 1800-1810, DOI: 10.1002/chem.201102151.

[7] T.S. King, W.J. Goretzke, B.C. Gerstein, *Dispersion of silica-supported copper catalysts determined by NMR of ^{63}Cu*, J. Catal. 107 (1987) 583-586, DOI: 10.1016/0021-9517(87)90324-1.

[8] E.N. Muhamad, R. Irmawati, Y.H. Taufiq-Yap, A.H. Abdullah, B.L. Kniep, F. Girgsdies, T. Ressler, *Comparative study of Cu/ZnO catalysts derived from different precursors as a function of aging*, Catal. Today 131 (2008) 118-124, DOI: 10.1016/j.cattod.2007.10.010.

[9] B.L. Kniep, T. Ressler, A. Rabis, F. Girgsdies, M. Baenitz, F. Steglich, R. Schloegl, *Rational design of nanostructured copper-zinc oxide catalysts for the steam reforming of methanol*, Angew. Chem. Int. Ed. 43 (2004) 112-115, DOI: 10.1002/anie.200352148.

[10] A. Kharchenko, V. Zholobenko, A. Vicente, C. Fernandez, H. Vezin, V. De Waele, S. Mintova, *Formation of copper nanoparticles in LTL nanosized zeolite: spectroscopic characterization*, Phys. Chem. Chem. Phys. 20 (2018) 2880-2889, DOI: 10.1039/c7cp07650a.

[11] R.M. Sullivan, H. Liu, D. Steve Smith, J.C. Hanson, D. Osterhout, M. Ciraolo, C.P. Grey, J.D. Martin, *Sorptive reconstruction of the $CuAlCl_4$ framework upon reversible ethylene binding*, J. Am. Chem. Soc. 125 (2003) 11065-11079, DOI: 10.1021/ja036172o.

[12] J.R. Sudduth, D.A. Keyworth, *Process for the purification of gas streams*, U.S. Patent 3,960,910, 1975.

[13] S. Greiser, M. Hunger, C. Jaeger, *^{29}Si{^{27}Al} TRAPDOR MAS NMR to distinguishes Q^n(mAl) sites in alumosilicates. Test case: Faujasite-type zeolites*, Solid State Nucl. Magn. Reson. 79 (2016) 6-10, DOI: 10.1016/j.ssnmr.2016.10.004.

[14] S. Hu, J.A. Reimer, A.T. Bell, *^{65}Cu NMR spectroscopy of Cu-exchanged ZSM-5 catalysts*, J. Phys. Chem. B 101 (1997) 1869-1871, DOI: 10.1021/jp9630380.

[15] K.T. Mueller, *Analytic solutions for the time evolution of dipolar-dephasing NMR signals*, J. Magn. Reson. Ser. A 113 (1995) 81-93, DOI: 10.1006/jmra.1995.1059.

[16] J. Wu, N. Kim, J.F. Stebbins, *Temperature calibration for high-temperature MAS NMR to 913 K: ^{63}Cu MAS NMR of CuBr and CuI, and ^{23}Na MAS NMR of $NaNbO_3$*, Solid State Nucl. Magn. Reson. 40 (2011) 45-50, DOI: 10.1016/j.ssnmr.2011.04.004.

[17] W. Zhang, B.E.G. Lucier, Y. Huang, *Understanding Cu(I) local environments in MOFs via $^{63/65}$Cu NMR spectroscopy*, Chem. Sci. 15 (2024) 6690-6706, DOI: 10.1039/d4sc00782d.

[18] Z. Pang, K.O. Tan, *A focus on applying $^{63/65}$Cu solid-state NMR spectroscopy to characterize Cu MOFs*, Chem. Sci. 15 (2024) 6604-6607, DOI: 10.1039/d4sc90069c.

[19] J.A. Tang, B.D. Ellis, T.H. Warren, J.V. Hanna, C.L.B. Macdonald, R.W. Schurko, *Solid-state ^{63}Cu and ^{65}Cu NMR spectroscopy of inorganic and organometallic copper(I) complexes*, J. Am. Chem. Soc. 129 (2007) 13049-13065; DOI: 10.1021/ja073238x.

[20] B.E.G. Lucier, J.A. Tang, R.W. Schurko, G.A. Bowmaker, P.C. Healy, J.V. Hanna, *Solid-state ^{65}Cu and ^{31}P NMR Spectroscopy of bis(triphenylphosphine) copper species*, J. Phys. Chem. C 114 (2010) 7949-7962, DOI: 10.1021/jp907477m.

[21] D. Rusanova, W. Forsling, O.N. Antzutkin, K.J. Pike, R. Dupree, *Solid-state ^{31}P CP/MAS and static ^{65}Cu NMR characterization of polycrystalline copper(I) dialkyldithiophosphate clusters*, J. Magn. Reson. 179 (2006) 140-145, DOI: 10.1016/j.jmr.2005.10.013.

[22] N. Yamakawa, M. Jiang, C.P. Grey, *Investigation of the conversion reaction mechanisms for binary copper(II) compounds by solid-state NMR spectroscopy and X-ray diffraction*, Chem. Mater. 21 (2009) 3162-3176, DOI: 10.1021/cm900581b.

[23] L.A. O'Dell, A. Rossini, R.W. Schurko, *Acquisition of ultra-wideline NMR spectra from quadrupolar nuclei by frequency stepped WURST–QCPMG*, Chem. Phys. Lett. 468 (2009) 330, DOI: 10.1016/j.cplett.2008.12.044.

[24] H. Yu, X. Tan, G.M. Bernard, V.V. Terskikh, J. Chen, R.E. Wasylishen, *Solid-state ^{63}Cu, ^{65}Cu, and ^{31}P NMR spectroscopy of photoluminescent copper(I) triazole phosphine complexes*, J. Phys. Chem. A 119 (2015) 8279-8293, DOI: 10.1021/acs.jpca.5b04270.